

Stabilized crack-opening stresses as a function of R-ratios and stress levels

Rahi Chermahini^{1*}, Majid Jabbari²

¹*Mobarakeh Steel Research Center, the core of fatigue and fracture in solids*

²*Department of Mechanical Engineering, Khomeinishahr Branch, Islamic Azad University, Isfahan, 84175-119, Iran*

*rgcher31@gmail.com

(Manuscript Received --- 02 June 2022; Revised --- 16 June 2022; Accepted --- 21 June 2022)

Abstract

An elastic-perfectly plastic middle crack tension aluminum 2024-T3 alloy was used under plane stress, plane strain and 3D analysis to determine stabilized crack-opening stresses for different R-ratios and stress levels. The stabilized crack-opening stresses of a 3D analysis locate between those values of plane stress and plane strain conditions. Using the above strategy, one can determine crack-opening stresses for any desired thickness value using interpolating scheme. Two and three dimensional programs were developed based on small strain elasticity theory incorporating linear strain isoparametric elements. The plasticity part of the analysis uses initial stress approach. The crack was extended one element size as the applied load reached the maximum value of each load cycle. Crack opening and closure stresses of nodes on the crack surface plane after some cyclic crack extensions are demonstrated. Based on the obtained results, for the three-dimensional finite-element analysis, the calculated stabilized crack opening stresses always locate between those of plane stress and plane strain conditions.

Keywords: Finite Element, Elastic-Plastic, Cracks, Opening Stress ,Crack Closure.

1- Introduction

The growth behavior of cracks in engineering components is a three-dimensional process. This behavior is affected by the closure of crack- surface planes, which depends on the state of stress. The closure phenomenon is associated with the plastic deformation left at the vicinity of the cracked body. Microscopically, the plastic deformation is furnished by means of dislocation movement in the highly stressed region of

the material. Since the discovery of closure by W. Elber [1], many researchers have explored the closure behavior of metallic materials using numerical and experimental efforts. The works of many researchers have shown that closure under plane stress is much larger than that under plane strain conditions. The closure behavior of a three-dimensional cracked body varies along the crack front and depends on the crack geometry, crack size,

stress level and imposed boundary conditions. The three-dimensional closure behavior of finite thickness plates for different flaw geometries are investigated under different loading conditions [2-11]. Mirgilani [12] concentrate on modeling and growing a crack during Tension Stress and calculate first stress intensity factor. The previous closure work of three-dimensional cracked body by Chermahini, et al [7] suggested a closure value between that of plane stress and plane strain conditions using the same loading conditions. Based on the above phenomenon, one can determine the closure behavior of three dimensional specimens having different thicknesses by means of interpolating scheme along with the closure values of plane stress, plane strain and three-dimensional stress analysis with a specified thickness value. Using the above procedure, the two and three-dimensional finite element programs were used to determine the stabilized crack-opening stresses of middle crack tension specimens under constant amplitude crack extensions for different R-ratios and stress levels. The plot of stabilized crack-opening stresses as a function of both stress ratios and thicknesses are constructed for any stress level. The crack-closure and crack opening profiles of nodes on the crack-surface plane after some crack extensions are demonstrated for unloading and reloading portions of load history.

2-Specimen Configuration and Loading

The three-dimensional middle-crack tension specimen Fig. 1 was used under constant amplitude crack extensions with different R-ratios and stress levels. The dimensions of the tensile bar specimen was $b=38.1\text{mm}$, $h=76.2\text{mm}$. The crack was extended one element size (0.02mm) at the

maximum applied stress of each load cycle. The initial crack length was 18.57mm . The modulus of elasticity E was 70000MPa , Poisson ratio was 0.3 and the effective yield stress was 345MPa (Aluminum 2024-T3 Alloy). The finite-element analysis was used on the middle-crack tension specimen subjected to boundary condition and loading as shown in Fig. 2. The finite-element mesh in the $z=0$ plane, is shown in Fig. 3.

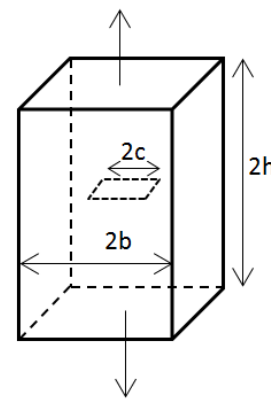


Fig. 1 Middle-crack tension specimen subjected to uniform stress

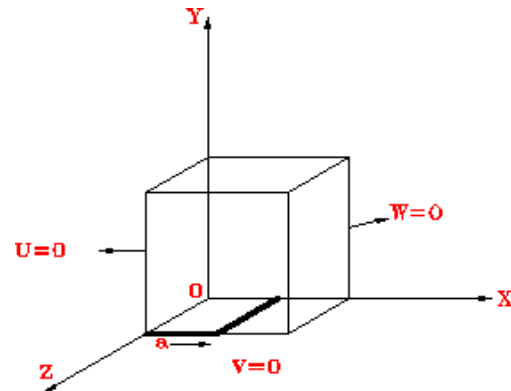


Fig. 2 A schematic of 1/8 of the middle- Crack tension specimen using finite-element analysis

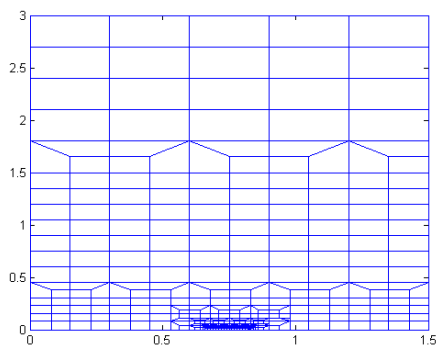


Fig. 3 Specimen idealizations in x-y plane

3-Results

The middle crack tension specimens were subjected to different R-ratios and stress levels using finite-element analyses of fatigue crack growth and closure. To acquire more information about the growth behavior of cracks on the fractured surfaces, two dimensional finite element analysis of fatigue crack growth and closure was applied to the middle crack tension specimens under stress level of 70MPa using different R-ratios. Then the three dimensional analysis was applied to the middle crack tension specimen under the same stress level and R-ratios. In the analysis, the $Z=0$ plane is considered as the interior region, whereas the $Z=C$ plane is considered the exterior one. In all of the models, the initial crack length was 18.57mm.

Using three-dimensional analysis, first the model was loaded to the maximum applied stress (70MPa) under $R=-1$. Then, the model was unloaded. During unloading, the nodes on the exterior region were closed. As the load was lowered, the other nodes on the crack-surface plane were closed. At the minimum applied stress, the nodes on the interior region were closed. As the model was reloaded, the nodes on the interior region were opened. As the load was increased further, the other nodes on the crack-surface plane were opened.

At the maximum applied stress, the last nodes on the exterior regions were opened. This procedure was repeated for a number of forty cycles. Then, the average stabilized crack-opening stresses for any R-ratios were determined.

As the previous work of three-dimensional fatigue crack closure [7] shows, the stabilized crack-opening stresses of a three-dimensional analysis always is between those of plane-stress and plane-strain conditions under the same loading history as shown in Fig. 4.

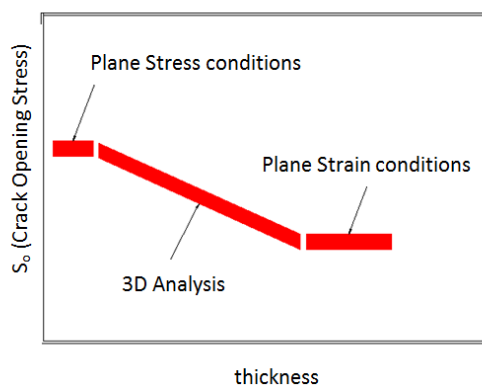


Fig. 4 Schematic diagrams of stabilized crack opening stresses as a function of thickness

Using this behavior, one can construct the stabilized crack-opening stresses for different thicknesses using simple interpolating scheme. The stabilized crack-opening stresses for stress level of 70MPa for Aluminum 2024-T3 alloy under different R-ratios are listed in Table. 1. The 3-D graph of opening stresses as a function of R-ratios and thicknesses are shown in Fig. 5.

To visualize the behavior of crack-closure and crack-opening stresses of nodes on the crack-surface plane, four different R-ratios (-1, -0.5, 0, 0.4) were chosen for the 30th cycle in the analysis. These behaviors of four different R-ratios are shown in Figs. 6–9, respectively.

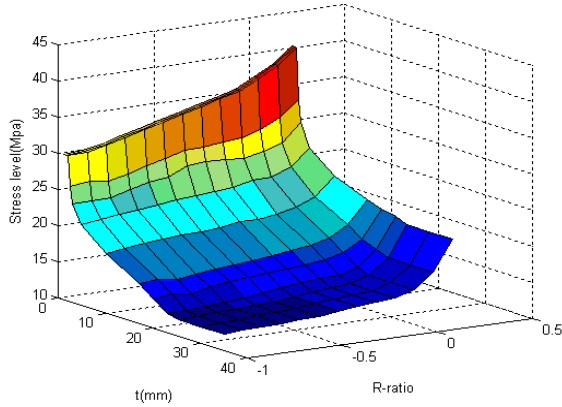


Fig. 5 Variation of stabilized crack opening stresses as a function of different thicknesses and stress ratios for stress level of 70MPa

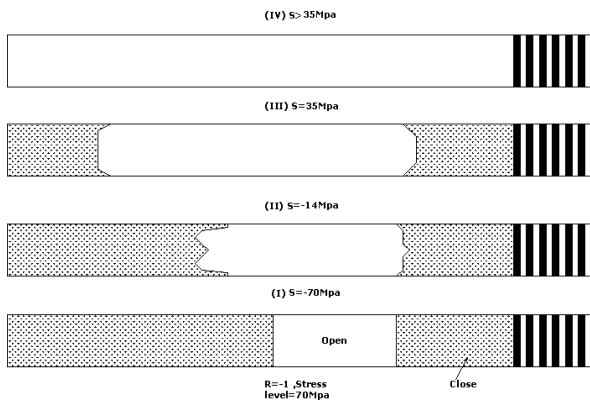


Fig. 6 Closure and opening profiles of nodes on the crack surface plane under constant-amplitude crack extension with $S_{max} = 0.2\sigma_{ys}$ and $R=-1$

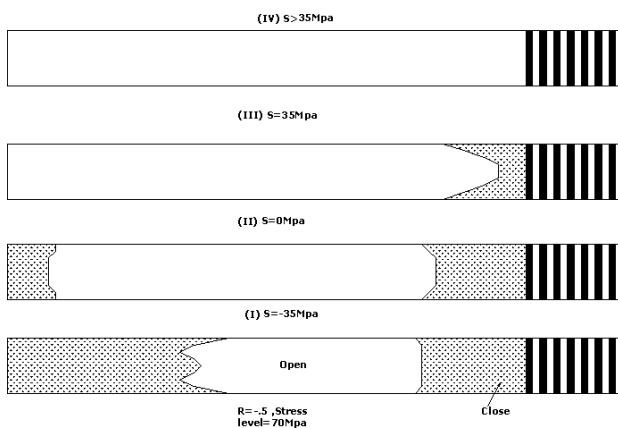


Fig. 7 Closure and opening profiles of nodes on the crack surface plane under constant-amplitude crack extension with $S_{max} = 0.2\sigma_{ys}$ and $R=-0.5$

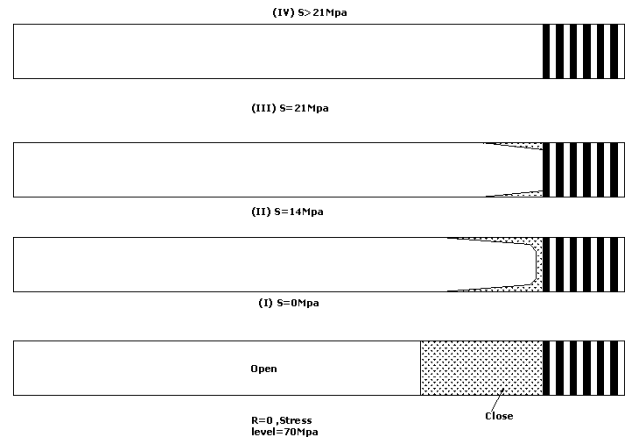


Fig. 8 Closure and opening profiles of nodes on the crack surface plane under constant-amplitude crack extension with $S_{max} = 0.2\sigma_{ys}$ and $R=0$

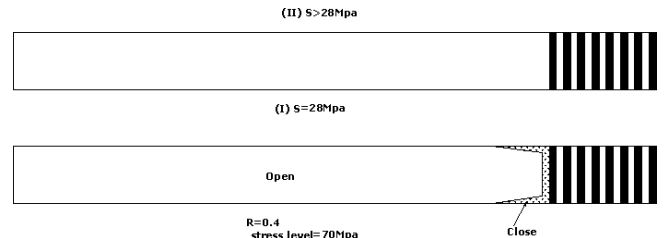


Fig. 9 Closure and opening profiles of nodes on the crack surface plane under constant-amplitude crack extension with $S_{max} = 0.2\sigma_{ys}$ and $R=0.4$

For $R=-1$, majority of nodes on the crack surface plane were closed and only some interior ones were opened. As the load was increased, the constraint effect on the interior region caused the interior nodes to be opened. Upon further increase in load, the other nodes on the interior of the crack-surface plane were opened. Beyond stress level of 35MPa, the entire crack-surface plane was fully opened.

For $R=-0.5$, most of the nodes on the crack-surface plane were closed and some interior ones were opened. This interior region is much larger than that of $R=-1$. As the load was increased further, the interior nodes due to the constraint effect were opened. At the stress level of 35MPa, some nodes in the vicinity of the crack were closed. Beyond this stress level, the entire crack- surface plane was fully opened.

For $R=0$, some nodes near the crack-tip region were closed. At stress level of 14MPa, only the nodes on the exterior regions were closed and the interior ones due to the constraint effect were opened. At stress level of 21MPa, only some nodes on the exterior region which are nearly under plane stress conditions were closed. Beyond that stress level, the entire crack-surface plane was fully opened.

For $R=0.4$, only some nodes on the exterior regions were closed. Beyond the stress level of 28MPa, the entire crack-surface plane was fully opened.

4-Conclusion

Two-and three-dimensional finite-element analysis of fatigue crack growth and closure were applied to the middle crack tension specimens under different R-ratios and stress levels using constant amplitude crack extensions. Based on the obtained results from the above analysis, the following conclusions can be drawn.

For the three-dimensional finite-element analysis, the calculated stabilized crack opening stresses always locate between those of plane stress and plane strain conditions.

For aluminum 2024 alloy, using damage tolerance procedures, having all the technical information regarding R-ratios and opening stresses and stress levels, one can determine the remaining life of engineering components. 3-Using plane strain conditions under stress level of 70 MPa for R ratios greater than 0.2, there was not observed any closure stresses.

References

[1] Newman, J. C. jr. (1998). The merging of fatigue and fracture mechanics concepts,

a historical perspective. *Progress in Aerospace science*, 34, 347-390.

[2] Newman, J. C. jr and Raju, I.S. (1984). Stress intensity factor equation for crack in three -dimensional finite bodies subjected to tension and bending loads. *NASA Technical Memorandum*, 85793.

[3] Elber, W. (1968). Fatigue crack propagation. *Ph.D. Thesis (University of New South Wales, Australia)*.

[4] Sih, G. C. and Chen, C. (1985). Non self-similar crack growth in elastic plastic -finite thickness plate. *Theor Appl Fract. Mech*, 3,125-139.

[5] Chermahini, R.G. (1986). Three-dimensional elastic-plastic finite element analysis of fatigue crack growth and closure. *Ph.D. Thesis (Old Dominion University, Norfolk, VA, August)*.

[6] Chermahini, R.G., Shivakumar, K.N. and Newman, J. C. jr. (1988). Three-dimensional finite-element simulation of fatigue crack growth and closure. *ASTMSTP 982 (American society for Testing and materials)*.

[7] Chermahini, R.G., Shivakumar, K.N. and Newman, J. C. jr and Blom, A. F. (1989). Three-dimensional aspects of plasticity induced fatigue crack closure. *Eng Frac Mech*, 34, 393-401.

[8] Chermahini, R.G. and Blom, A.F. (1991). Variation of crack opening stresses in three-dimensional finite thickness plate. *Theor Appl Fract Mech*, 15, 267-276.

[9] Chermahini, R.G., Palmberg, B. and Blom, A.F. (1993). Fatigue crack growth and closure behavior of semicircular and elliptical surface flaws. *Int J Fatigue*, 4, 259-263.

[10] Chermahini, R.G. (2003). Fatigue crack growth and closure behavior of

surface flaws under different R-ratios.
Proceeding of the 4th Iranian aerospace Society Conference, 87-98.

[11] Chermahini, R.G. (2004). Fatigue crack growth and closure behavior of circular and elliptical edge cracks. *The Fifth national Conference of Iranian Aerospace Society*, 325-329.

[12] Hossein Mirgilani, S.M. (2013). Modeling and crack-growth and calculate first intensity factor with ANSYS software. *Journal of Simulation and Analysis of Novel Technologies in Mechanical Engineering*, 2(4), 49-53.

.